

Structure of duplex DNA containing the cisplatin 1,2- $\{\text{Pt}(\text{NH}_3)_2\}^{2+}$ -d(GpG) cross-link at 1.77 Å resolution

(For submission to *J. Inorg. Biochem.*)

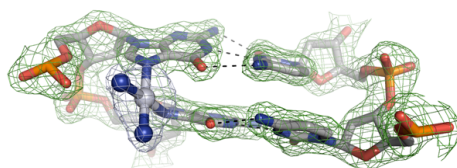
Ryan C. Todd^a and Stephen J. Lippard^{a*}

^aDepartment of Chemistry, Massachusetts Institute of Technology, 77 Massachusetts Avenue, Cambridge, MA 02139

*To whom correspondence should be addressed. E-mail: lippard@mit.edu, Phone: 617.253.1892, Fax: 617.258.8150

R.C.T. designed and performed experiments, and wrote the paper. S.J.L. designed experiments and wrote the paper.

Table of Contents Graphic



Synopsis

The structure of a cisplatin-modified DNA dodecamer duplex containing a 1,2-*cis*- $\{\text{Pt}(\text{NH}_3)_2\}^{2+}$ -d(GpG) cross-link has been determined at 1.77-Å resolution. Improved electron density reveals new features not seen in the originally published 2.6 Å structure.

Abstract

We report the 1.77-Å resolution X-ray crystal structure of a dodecamer DNA duplex with the sequence 5'-CCTCTGGTCTCC-3' that has been modified to contain a single engineered 1,2-*cis*-{Pt(NH₃)₂}²⁺-d(GpG) cross-link, the major DNA adduct of cisplatin. These data represent a significant improvement in resolution over the previously published 2.6-Å structure. The ammine ligands in this structure are clearly resolved, leading to improved geometry of the cross-link. Other new features of this model include the location of four octahedral [Mg(H₂O)₆]²⁺ complexes associated with bases in the DNA major groove and the identification of 124 additional ordered water molecules that participate in hydrogen bonding interactions with either the nucleic acid or the diammineplatinum(II) moiety. The global DNA geometry is overall very similar between the current and originally determined structures.

Keywords

cisplatin, DNA structure, X-ray crystallography

1. Introduction

Platinum-based therapy remains a highly utilized and effective option in the treatment of many types of cancer [1]. After cisplatin (*cis*-diamminedichloroplatinum(II)) was discovered to have antitumor properties more than 40 years ago [2, 3], much research has focused on unraveling the mode of action of this compound. Nuclear DNA is a molecular target for platinum anticancer compounds, which bind purine bases at the N7 position. The resulting Pt-DNA damage triggers downstream effects including

inhibition of replication and transcription, cell cycle arrest, and attempted repair of the damaged nucleotides. If the cell cannot remove the damage then it dies by one of several pathways [4].

Revealing the structural details of Pt-DNA adducts represented a significant milestone in platinum anticancer research. This information has helped to build structure-activity relationships that underlie transcription inhibition and cell death. The major adduct of cisplatin-DNA binding is a 1,2-intrastrand adduct between adjacent guanine bases; a minor percentage of 1,3-intrastrand and interstrand cross-links also form [4]. The 1,2-d(GpG) cisplatin cross-link was first characterized crystallographically in a DNA dodecamer duplex in 1996 at 2.6-Å resolution. This structure revealed that the Pt adduct induces a global bend of 35-40° in the DNA duplex and unwinds the double helix by ~25° [5, 6]. The major groove is compacted and the minor groove widened and flattened. A-form DNA comprises the nucleic acid to the 5' side of the Pt cross-link, and B-DNA forms to the 3' side of the 1,2-d(GpG) adduct. The roll angle between platinated guanine bases is 26° and, as a consequence, results in considerable strain being placed on the Pt-N7 bonds, displacing the Pt atom out of the guanine ring planes by approximately 1 Å each.

In the present article we report a higher resolution, 1.77 Å structure of this complex, a dodecamer duplex having the sequence 5'-CCTCTG*G*TCTCC-3', where the asterisks denote platination sites. This significant increase in resolution offers a much-improved view of the molecule, especially in the Pt-DNA adduct region. Pt-N bond distances and angles for the present model now match closely the values expected for a square-planar Pt coordination compound. Also located in the current

structure are four octahedral $[\text{Mg}(\text{H}_2\text{O})_6]^{2+}$ complexes that interact with the DNA duplex through the primary hydration sphere, and ordered water molecules that hydrogen bond to both the nucleic acid and the $\{\text{Pt}(\text{NH}_3)_2\}^{2+}$ unit. The global DNA geometry remains relatively unchanged compared to that of the original structure. These new, high resolution results reveal valuable structural features of the cisplatin 1,2-*cis*- $\{\text{Pt}(\text{NH}_3)_2\}^{2+}$ -d(GpG) cross-link on DNA not previously attainable.

2. Materials and Methods

Phosphoramidites, columns, and other reagents for solid-phase oligonucleotide synthesis were purchased from Glen Research. Potassium tetrachloroplatinate(II), which was used to synthesize cisplatin according to published procedures [7], was a gift from Engelhard (Iselin, NJ, now BASF). Crystallization reagents and supplies were obtained from Hampton Research. All other reagents were purchased from commercial suppliers and used without further purification. Oligonucleotides were prepared in-house using an Applied Biosystems Model 392 DNA/RNA Synthesizer. Liquid chromatography was performed with an Agilent 1200 series HPLC equipped with a temperature-controlled autosampler and automated fraction collector. Atomic absorption spectroscopy was performed with a Perkin Elmer AAnalyst 300 system. UV-Vis spectra were collected on a Hewlett-Packard 8453 spectrophotometer.

2.1. Preparation of platinated DNA duplex

The oligonucleotide 5'-d(CCTCTGGTCTCC)-3' (**1**) and its complement (**2**) were synthesized on a 2x1.0 μmol scale with dimethoxytrityl (DMT) groups on by standard

solid-phase synthetic methods. The strands were purified by reversed-phase high-pressure liquid chromatography (HPLC) on an Agilent SB-300, 9.4 x 250 mm column, with a linear gradient of 100 mM triethylammonium acetate pH 7.0 and acetonitrile. After lyophilization of combined fractions, DMT groups were removed in 80% acetic acid for 30 min at room temperature, and the oligonucleotides were precipitated with isopropanol and desalted with Waters Sep-Pak C18 cartridges. Reaction of **1** with 1.2 equiv of cisplatin was carried out in 10 mM HEPES pH 6.8 buffer for 14 h at 37 °C. Platinated product was purified by ion-exchange HPLC on a Dionex DNA-Pac PA-100, 9.4 x 250 mm column at 35 °C, with a mobile phase of 90:10 25 mM Na acetate pH 5.2:acetonitrile and a linear NaCl gradient. Combined peak fractions were dialyzed against water overnight, then lyophilized and reconstituted in water, yielding 5'-d(CCTCTG*G*TCTCC)-3' (**3**). The site-specifically platinated duplex was prepared by combining equimolar amounts of **3** and **2** in 200 µL of 200 mM LiCl, 100 mM HEPES pH 7.0, and 50 mM MgCl₂, heating to 70 °C for 10 min, and cooling to 4 °C over 2.5 h. The duplex was purified by ion exchange HPLC as described above but with a LiCl gradient. The final product was dialyzed, lyophilized, and desalted as described above.

2.2 Crystallization and X-ray diffraction data collection

Diffraction-quality crystals were grown by hanging-drop vapor diffusion at 4 °C. Crystallization solutions contained 120 mM magnesium acetate, 50 mM sodium cacodylate pH 6.5, 1 mM spermine, and 28% w/v polyethylene glycol (PEG) 4000; hanging drops contained 2 µL of 0.4 mM Pt-DNA in water and 2 µL of crystallization solution, equilibrated against 1 mL of crystallization solution. All solutions were prepared

and sterile filtered immediately before use. Crystals with dimensions of ~1.0 mm x 0.2 mm x 0.1 mm grew in clusters in approximately two weeks.

Single crystals were isolated from the clusters and transferred to a cryoprotectant solution of 120 mM magnesium acetate, 50 mM sodium cacodylate pH 6.5, 1 mM spermine, 28% w/v polyethylene glycol (PEG) 4000, and 15% v/v glycerol, mounted on loops, and flash frozen directly in liquid nitrogen. Diffraction data were collected at 100 K ($\lambda = 0.979 \text{ \AA}$) at beamline 9-2 of the Stanford Synchrotron Radiation Laboratory (SSRL), and processed in HKL2000 [8]. Data were collected over 360° with 1° oscillation per frame. Data collection statistics are shown in **Table 1**.

2.3. Structure determination

Phasing of the diffraction data was achieved by molecular replacement with the program Phaser [9] using the original structure (1AIO) with all water molecules removed as a search model. After one round of refinement with Refmac5 [10], the R_{free} value was below 24%. Platinum-nitrogen bond distances and angles were adjusted to fit the improved electron density around the ammine ligands, and $[\text{Mg}(\text{H}_2\text{O})_6]^{2+}$ sites were inserted manually into the $2F_o - F_c$ and $F_o - F_c$ electron density maps with the program Coot [11]. Water molecules were placed automatically with Coot into areas of $F_o - F_c$ density above 3.5σ and then adjusted manually. Subsequent rounds of refinement and model adjustment were performed to afford the final model with an R_{free} value of 20.9%. Final refinement statistics are given in **Table 1**. Nucleic acid geometric parameters were calculated with the program 3DNA [12]. Single point energy calculations were performed with Gaussian 03 suite of programs [13]. From the experimental structures,

the atomic valences were completed with hydrogen atoms. Thus, the final model carries a molecular charge of 2+. In this approach, the models are treated by Density Functional Theory (DFT), with the B3LYP functional [14, 15] and the 6-31g(d,p) basis set [16] on all light atoms (H, C, N, O and P). Platinum was represented by the Los Alamos LANL2DZ basis [17, 18], which includes relativistic effective core potentials. All crystallographic images in this paper were created using Pymol [19]. Coordinates have been deposited into the Protein Data Bank (PDB) with accession code XXXX.

3. Results and discussion

3.1 Unit cell and crystal packing

Crystals of the Pt-DNA construct were grown under different conditions than those reported from the original investigation; however, the two structures are nearly identical. The present conditions were used to obtain diffraction quality crystals of DNA duplexes containing an oxaliplatin-DNA cross-link [20] as well as a monofunctional Pt-DNA adduct of *cis*-diammine(pyridine)chloroplatinum(II) [21]. Despite the difference in the present and previous conditions used to grow crystals, the cisplatin-modified duplex DNA crystallizes in the same space group, *P1*, and with nearly identical unit cell dimensions as the previous structure. Unit cell dimensions for the original crystal structure are $a = 31.27 \text{ \AA}$, $b = 35.46 \text{ \AA}$, $c = 47.01 \text{ \AA}$, $\alpha = 79.81^\circ$, $\beta = 84.75^\circ$, and $\gamma = 82.79^\circ$, whereas the dimensions for this crystal are $a = 31.30 \text{ \AA}$, $b = 35.43 \text{ \AA}$, $c = 45.13 \text{ \AA}$, $\alpha = 80.06^\circ$, $\beta = 84.09^\circ$, and $\gamma = 81.77^\circ$, giving unit cell volumes of $50,770 \text{ \AA}^3$ and $48,729 \text{ \AA}^3$, respectively. The 4% decrease in volume can be attributed to differences in temperature; data for the first cisplatin-DNA structure were collected at 277 K, whereas

we collected the current data at 100 K. Because the unit cells are nearly equivalent, packing interactions between molecules are also conserved between structures. Two unique DNA duplexes comprise the asymmetric unit that are related by non-crystallographic symmetry and interact via hydrogen bonding, end-to-end, and end-to-groove contacts in the crystal lattice. The combination of the latter two interactions in the same crystal is unusual, the former being typically observed in B-form DNA structures and the latter in crystals of A-form nucleic acids. As a possible consequence of these packing interactions, this cisplatin-modified DNA structure displays a unique characteristic that is absent in other structural studies of the 1,2-*cis*-{Pt(NH₃)₂}²⁺-d(GpG) cross-link in double stranded DNA, namely, considerable angular strain at the Pt–N7 bonds. As a consequence, the platinum atom lies out-of-plane of the guanine bases by ~1 Å each. This feature was noted in the original structure but was not analyzed in detail. Our high-resolution data confirm its presence in the structure and facilitates a thorough examination of its origin (*vide infra*).

3.2. Global DNA geometry

Notable characteristics of DNA containing the cisplatin 1,2-{Pt(NH₃)₂}²⁺-d(GpG) cross-link, determined from the original crystal structure, include bending of the double helix by 35-40° toward the major groove and local duplex unwinding of ~25°. The roll angle between Pt-bound guanine bases is 26°, and the DNA takes on A-form properties on the 5' side of the Pt-DNA adduct, and B-form structure on the 3'-end [6]. However, the resolution limit prohibited direct visualization of deoxyribose sugar puckers, so ring conformations were indirectly determined by measuring distances between adjacent

phosphate atoms and examining base-stacking patterns. The same structural features are present in the current 1.77 Å structure (see **Figs. 1a** and **S1**), but the sugar ring conformations can be differentiated as either C2' endo (typical of A-form DNA) or C3' endo (for B-form DNA) by visualization of the electron density. DNAs from the previous and current models align nearly identically, with a root-mean-square deviation (rmsd) over all atoms of 0.472 Å (see **Fig. 2**). Although there are two molecules in the unit cell, the DNA structures of each are also equivalent, with a rmsd over all atoms of 0.18 Å. A detailed analysis of the global DNA structure will not be discussed here; it can be found in the original publication [6].

3.3. Pt adduct geometry

Unlike the overall DNA structure that is unchanged by addition of higher resolution diffraction data, the cisplatin adduct is significantly altered in the current model. Clear electron density is now visible for the ammine ligands of the 1,2-*cis*-{Pt(NH₃)₂}²⁺-d(GpG) cross-link (see **Fig. 1b**), allowing the square-planar Pt geometry to be accurately evaluated. The Pt–N bond lengths for all four ligands average to 2.02 Å in the new model, compared to 1.90 Å in the previous structure, and 2.02 Å in the X-ray crystal structure of the 1,2-*cis*-{Pt(NH₃)₂}²⁺-d(GpG) dinucleotide determined at atomic resolution [22]. The average *cis* N–Pt–N angles for the current and prior models and the dinucleotide structure are 90.0°, 88.0°, and 90.0° respectively, with ranges of 83.9° - 99.8°, 70.9° - 99.9°, and 86.9° - 94.3°, respectively. The *trans* angles are dramatically improved in the high-resolution model, with an average N–Pt–N value of 174.5°, compared to 156.9° in the 2.6 Å-resolution model and 175.1° for the isolated Pt-d(GpG)

cross-link. Thus the current model depicts a platinum adduct geometry that very nearly matches that observed in the X-ray crystal structure of the 1,2-*cis*-{Pt(NH₃)₂}²⁺-d(GpG) dinucleotide. A full comparison of Pt geometries is provided in **Table 2**.

Consistent with the original model, the platinum atoms are displaced from the guanine base planes. The metal atom lies out-of-plane of the 5' guanine by 1.2 and 1.1 Å in the two molecules, and of the 3' nucleobase by 1.0 Å in both DNA duplexes. This feature, however, is inconsistent with data from both the X-ray crystal structure of the 1,2-*cis*-{Pt(NH₃)₂}²⁺-d(GpG) dinucleotide [22] and the NMR solution structure of duplex DNA containing the lesion [23], in which the Pt atom is located within the guanine base planes and the dihedral angle between bases is ~90° (see **Fig. 3**). The shallow roll angle in the present X-ray crystal structure causes significant angular strain on the Pt–N7 bonds. Single point energy calculations indicate that the {Pt(NH₃)₂}²⁺-d(GpG) moiety in the Pt-DNA X-ray structure is 14.6 kcal/mol higher in energy than the analogous NMR solution structure [23]. DNA end-to-end packing on the 3' side of the Pt adduct and end-to-groove packing on the 5' side of the cross-link appear to dictate the global curve of the molecule and prevent complete opening of the guanine-guanine base pair roll angle. However, the same crystal packing contacts are capable of stabilizing the altered higher energy conformation, since a single hydrogen bonding interaction can contribute ca. 1 - 9 kcal/mol in energy [24]. These results underscore the importance of evaluating macromolecular structures by multiple means, including NMR spectroscopy and biochemical methods in addition to X-ray crystallography, because each has its limitations.

3.4. Magnesium sites identified

Four fully aquated magnesium(II) cations were located in the major groove on the A-form side of the nucleic acid double helix. As in other DNA crystal structures, interaction of the $\text{Mg}(\text{aq})^{2+}$ cation and the DNA major groove occurs via hydrogen bonding, the water ligands serving as hydrogen bond donors to the N7 atoms of guanine and adenine bases and to the O6 atom of guanine (see **Fig. 1c**) [25, 26]. In all cases the $[\text{Mg}(\text{H}_2\text{O})_6]^{2+}$ cations interact with adjacent purine bases, either the terminal d(GpG) or the d(ApG) dinucleotide sequence at the 3' end of the unplatinated strand (see **Fig. 4**).

Significantly better electron density exists for two $\text{Mg}(\text{aq})^{2+}$ complexes bound to the terminal d(GpG) sequence than the other two sites. Crystallographic B-factors for the former are 39.1 and 38.1 \AA^2 , compared to 53.4 and 49.2 \AA^2 for the latter. The d(GpG)-bound $[\text{Mg}(\text{H}_2\text{O})_6]^{2+}$ complexes contribute four hydrogen bonding interactions with the DNA bases, whereas the less ordered sites participate in only three such contacts. This difference is one possible reason why the first two sites have lower B-factors. As a result, the Mg–OH₂ bond distances for the former, which average 2.05 ± 0.08 \AA , are close to the reported literature values of 2.06 \AA [26], and the complexes have nearly ideal octahedral symmetry. The magnesium(II) complexes that bind d(ApG) sequences near the platinum adduct, bases 20-21 and 44-45 as depicted in **Fig. 5**, have Mg–OH₂ bond distances as long as 2.46 \AA if left unrestrained (data not shown), which is clearly unrealistic and an artifact of insufficiently well defined electron density around those water ligands. These complexes were therefore refined with restraints on bond distances and angles, whereas the d(GpG) coordinated $\text{Mg}(\text{aq})^{2+}$ sites were

refined without restraints. No $[\text{Mg}(\text{H}_2\text{O})]^{2+}$ -DNA interactions were observed at the B-form end of this palindromic sequence, although they are probably present but not visible in the electron density. Average crystallographic B-factors for the four terminal base pairs on the 5' side of the Pt cross-link, where $\text{Mg}(\text{aq})^{2+}$ coordination is resolved, are 33.4 and 34.6 \AA^2 for the two DNA duplexes. In contrast, these values are 44.4 and 44.5 \AA^2 for the last four base pairs on the 3' ends of the two molecules, indicating that the B-form sections of each nucleic acid are less ordered than the respective A-DNA segments.

3.5. Ordered water molecules

Of the 148 ordered water molecules located in the model, 24 are bound to magnesium in an octahedral geometry as described above. The remaining 124 solvent molecules interact with either the platinum adduct, phosphodiester backbone, or the DNA bases. A schematic depiction of each of these solvent-DNA interactions is given in **Fig. 5**, and a full list of water contacts appears in **Table S1**. One water molecule participates in bridging hydrogen-bonding interactions with each of the platinum ammine ligands. Molecule A has four solvent molecules bound to the Pt-DNA adduct, whereas molecule B has only two ammine-bound waters. Unlike another high-resolution structure of Pt-modified DNA, no direct interaction between ordered waters and the platinum atom is observed [27, 28].

Hydrogen bonding interactions between water molecules and nucleobases occur primarily at guanine N7, O6, or N3 atoms, adenine N7, N6, or N3, thymine O2 or O4, and cytosine N4 or O2 positions, consistent with previous observations of Watson-Crick base pair hydration patterns [29, 30]. Water contacts with oxygen atoms of the

deoxyribose rings (O3', O4', or O5') are also observed, although less regularly. There are more resolved water-nucleobase interactions at the central base pairs in the duplexes; terminal base pairs do not show as much detail in the hydration sphere, presumably due to increased thermal motion.

The phosphodiester backbone of each DNA double helix is extensively hydrated, with water molecules participating in hydrogen bonding with the phosphate oxygen atoms. Mono- and bidentate interactions, either with two oxygen atoms from a single phosphate or from adjacent nucleotides, occur. Most bridging interactions between two phosphates are found in the central four base pairs, where the DNA backbone structure is distorted by the cisplatin cross-link. Some of the atoms modeled here as oxygen from water may actually be sodium ions, given that 50 mM sodium cacodylate was present in the crystallization buffer and that DNA exists as a polyanion and must be neutralized by cations. However, these two species cannot be differentiated by X-ray crystallography since Na^+ and O^{2-} each contain ten electrons; therefore, all non-magnesium solvent molecules were modeled as water.

4. Conclusions

The structure of a dodecamer DNA duplex containing a centrally located 1,2-*cis*- $\{\text{Pt}(\text{NH}_3)_2\}^{2+}$ -d(GpG) intrastrand cross-link of cisplatin was determined by X-ray crystallography to 1.77 Å resolution, a greater than 0.8 Å improvement over the previous structure solved in 1996. The improvement in resolution allowed us to model accurately the structure of the platinum adduct, which now closely matches its anticipated square-planar geometry, as well as to discover octahedral magnesium sites

at multiple locations in the DNA major groove. Hydrogen bonding interactions from 148 solvent water molecules were resolved here, compared with only 31 in the original structure.

Understanding the structural changes to DNA that occur upon binding of platinum antitumor agents is a critical step in deciphering the mechanism of these compounds. X-ray crystallography is a powerful technique for answering some of these questions, and should continue to be relied upon in the future as other platinum complexes are synthesized and studied. From these data we can better understand how Pt-DNA adducts might be repaired and inhibit cellular transcription. Understanding these two functions is key to the design of improved platinum candidates for cancer chemotherapy.

Acknowledgements

This work was supported by the National Cancer Institute (grant CA034992 to SJL). RCT is grateful for a Koch Fund fellowship from the Koch Institute for Integrative Cancer Research at MIT. We thank Engelhard Corporation (now BASF) for the generous donation of K_2PtCl_4 used in this research and Juliana Fedoce Lopes for conducting single point energy calculations. Portions of this research were carried out at the Stanford Synchrotron Radiation Laboratory, a national user facility operated by Stanford University on behalf of the U.S. Department of Energy, Office of Basic Energy Sciences. The SSRL Structural Molecular Biology Program is supported by the Department of Energy, Office of Biological and Environmental Research, and by the National Institutes

of Health, National Center for Research Resources, Biomedical Technology Program, and the National Institute of General Medical Sciences.

References

- [1] L. Kelland, *Nat. Rev. Cancer* 7 (2007) 573-584.
- [2] B. Rosenberg, L. Van Camp, T. Krigas, *Nature* 205 (1965) 698-699.
- [3] B. Rosenberg, L. Van Camp, J.E. Trosko, V.H. Mansour, *Nature* 222 (1969) 385-386.
- [4] D. Wang, S.J. Lippard, *Nat. Rev. Drug Discovery* 4 (2005) 307-320.
- [5] P.M. Takahara, A.C. Rosenzweig, C.A. Frederick, S.J. Lippard, *Nature* 377 (1995) 649-652.
- [6] P.M. Takahara, C.A. Frederick, S.J. Lippard, *J. Am. Chem. Soc.* 118 (1996) 12309-12321.
- [7] S.C. Dhara, *Indian J. Chem.* 8 (1970) 193-194.
- [8] Z. Otwinowski, W. Minor, *Methods Enzymol.* 276 (1997) 307-326.
- [9] A.J. McCoy, R.W. Grosse-Kunstleve, P.D. Adams, M.D. Winn, L.C. Storoni, R.J. Read, *J. Appl. Cryst.* 40 (2007) 658-674.
- [10] G.N. Murshudov, A.A. Vagin, E.J. Dodson, *Acta Crystallogr. D*53 (1997) 240-255.
- [11] P. Emsley, K. Cowtan, *Acta Crystallogr. D*60 (2004) 2126-2132.
- [12] X.-J. Lu, W.K. Olson, *Nucleic Acids Res.* 31 (2003) 5108-5121.
- [13] M.J. Frisch, H.B.S. G. W. Trucks, G. E. Scuseria,, J.R.C. M. A. Robb, J. A. Montgomery, Jr., T. Vreven,, J.C.B. K. N. Kudin, J. M. Millam, S. S. Iyengar, J. Tomasi,, B.M. V. Barone, M. Cossi, G. Scalmani, N. Rega,, H.N. G. A. Petersson, M. Hada, M. Ehara, K. Toyota,, J.H. R. Fukuda, M. Ishida, T. Nakajima, Y. Honda, O. Kitao,, M.K. H. Nakai, X. Li, J. E. Knox, H. P. Hratchian, J. B. Cross,, C.A. V. Bakken, J. Jaramillo, R. Gomperts, R. E. Stratmann,, A.J.A. O. Yazyev, R. Cammi, C. Pomelli, J. W. Ochterski,, K.M. P. Y. Ayala, G. A. Voth, P. Salvador, J. J. Dannenberg,, S.D. V. G. Zakrzewski, A. D. Daniels, M. C. Strain,, D.K.M. O. Farkas, A. D. Rabuck, K. Raghavachari,, J.V.O. J. B. Foresman, Q. Cui, A. G. Baboul, S. Clifford,, B.B.S. J. Cioslowski, G. Liu, A. Liashenko, P. Piskorz,, R.L.M. I. Komaromi, D. J. Fox, T. Keith, M. A. Al-Laham,, A.N. C. Y. Peng, M. Challacombe, P. M. W. Gill,, W.C. B. Johnson, M. W. Wong, C. Gonzalez, and J. A. Pople, Gaussian, Inc. Wallingford CT (2004).

- [14] C. Lee, W. Yang, R.G. Parr, *Phys. Rev. B* 37 (1988) 785-789.
- [15] A.D. Becke, *J. Chem. Phys.* 98 (1993) 5648-5652.
- [16] W.J. Hehre, R. Ditchfield, J.A. Pople, *J. Chem. Phys.* 56 (1972) 2257-2261.
- [17] P.J. Hay, W.R. Wadt, *J. Chem. Phys.* 82 (1985) 299-310.
- [18] P.J. Hay, W.R. Wadt, *J. Chem. Phys.* 82 (1985) 270-283.
- [19] W.L. DeLano, DeLano Scientific, Palo Alto, CA, USA (2002).
- [20] B. Spingler, D.A. Whittington, S.J. Lippard, *Inorg. Chem.* 40 (2001) 5596-5602.
- [21] K.S. Lovejoy, R.C. Todd, S. Zhang, M.S. McCormick, J.A. D'Aquino, J.T. Reardon, A. Sancar, K.M. Giacomini, S.J. Lippard, *Proc. Natl. Acad. Sci. U.S.A.* 105 (2008) 8902-8907.
- [22] S.E. Sherman, D. Gibson, A.H.J. Wang, S.J. Lippard, *J. Am. Chem. Soc.* 110 (1988) 7368-7381.
- [23] L.G. Marzilli, J.S. Saad, Z. Kuklenyik, K.A. Keating, Y. Xu, *J. Am. Chem. Soc.* 123 (2001) 2764-2770.
- [24] D. Bandyopadhyay, D. Bhattacharyya, *Biopolymers* 83 (2006) 313-325.
- [25] M. Soler-López, L. Malinina, J.A. Subirana, *J. Biol. Chem.* 275 (2000) 23034-23044.
- [26] J.A. Subirana, M. Soler-Lopez, *Ann. Rev. Biophys. Biomol. Struct.* 32 (2003) 27-45.
- [27] F. Coste, J.-M. Malinge, L. Serre, W. Shepard, M. Roth, M. Leng, C. Zelwer, *Nucleic Acids Res.* 27 (1999) 1837-1846.
- [28] F. Coste, W. Shepard, C. Zelwer, *Acta Crystallogr. D* 58 (2001) 431-440.
- [29] B. Schneider, D.M. Cohen, L. Schleifer, A.R. Srinivasan, W.K. Olson, H.M. Berman, *Biophys. J.* 65 (1993) 2291-2303.
- [30] H.M. Berman, *Biopolymers* 44 (1997) 23-44.

Figure Captions

Figure 1. Structural features of cisplatin-damaged DNA. (a) Overall structure of duplex DNA containing a cisplatin cross-link (shown in white/gray). (b) Stereo images of the

platinum-bound base pairs in molecule A with $2F_o-F_c$ electron density (green around the DNA/blue around the Pt adduct) contoured at 1.5σ . (c) Stereo images of a $[\text{Mg}(\text{H}_2\text{O})_6]^{2+}$ octahedral site bound in the major groove of molecule A at guanine residues 23 and 24, with $2F_o-F_c$ electron density (shown in blue) contoured at 1.5σ .

Figure 2. Stereo view of molecule A of the previously published structure of DNA modified with a 1,2-*cis*- $\{\text{Pt}(\text{NH}_3)_2\}^{2+}$ -d(GpG) cross-link (PDB accession code 1AIO, shown in blue) superimposed on the current high-resolution structure (XXXX, in red). The two molecules align almost identically, with a rmsd over all atoms of 0.472 Å.

Figure 3. Views of the 1,2-*cis*- $\{\text{Pt}(\text{NH}_3)_2\}^{2+}$ -d(GpG) adduct as depicted by (a) the X-ray crystal structure of the isolated dinucleotide [22], (b) the NMR solution structure of the Pt moiety in 8-mer duplex DNA [23], and (c) the X-ray crystal structure determination of dodecamer DNA presented here.

Figure 4. Binding of $[\text{Mg}(\text{H}_2\text{O})_6]^{2+}$ cations to purine dinucleotides in the cisplatin-DNA dodecamer duplex. Hydrogen bonding interactions between water ligands and nucleobases are depicted in cyan.

Figure 5. Schematic depicting hydrogen-bonding interactions between solvent molecules and Pt-DNA. For clarity, many contacts between water molecules are omitted.